STARS

University of Central Florida
STARS

Faculty Bibliography 2010s

Faculty Bibliography

1-1-2010

Temperature dependence of binary and ternary recombination of D-3(+) ions with electrons

T. Kotrík

P. Dohnal

I. Korolov

R. Plašil

Š. Roučka

See next page for additional authors

Find similar works at: https://stars.library.ucf.edu/facultybib2010

University of Central Florida Libraries http://library.ucf.edu

Recommended Citation

University of
Central
Florida

STARS
Showcase of Text, Archives, Research & Scholarship

Authors

T. Kotrík, P. Dohnal, I. Korolov, R. Plašil, Š. Roučka, J. Glosík, Chris H. Greene, and V. Kokoouline

Temperature dependence of binary and ternary recombination of D_3^+ ions with electrons

T. Kotrík, P. Dohnal, I. Korolov, R. Plašil, Š. Roučka, J. Glosík, Chris H. Greene, and V. Kokoouline

ARTICLES YOU MAY BE INTERESTED IN

133, 034305

Temperature dependence of binary and ternary recombination of D$_3^+$ ions with electrons

T. Kotrík,[1] P. Dohnal,[1] I. Korolov,[1] R. Plašil,[1,a)] Š. Roučka,[1] J. Glosík,[1] Chris H. Greene,[2] and V. Kokoouline[3,4]

[1]*Faculty of Mathematics and Physics, Charles University, 12116 Prague, Czech Republic*
[2]*Department of Physics and JILA, University of Colorado, Boulder, Colorado 80309-0440, USA*
[3]*Department of Physics, University of Central Florida, Orlando, Florida 32816, USA*
[4]*Laboratoire Aimé Cotton, CNRS, Université Paris-Sud XI, 91405 Orsay, France*

Flowing and stationary afterglow experiments were performed to study the recombination of D$_3^+$ ions with electrons at temperatures from 77 to 300 K. A linear dependence of apparent (effective) binary recombination rate coefficients on the pressure of the helium buffer gas was observed. Binary (D$_3^+$+e^-) and ternary (D$_3^+$+e^-+He) recombination rate coefficients were derived. The obtained binary rate coefficient agrees with recent theoretical values for dissociative recombination of D$_3^+$. We describe the observed ternary process by a mechanism with two rate determining steps. In the first step, a rotationally excited long-lived neutral D$_3^*$ is formed in D$_3^+$−e^- collisions. As the second step, the D$_3^*$ collides with a helium atom that prevents autoionization of D$_3^*$. We calculate lifetimes of D$_3^*$ formed from ortho-, para-, or metastates of D$_3^+$ and use the lifetimes to calculate ternary recombination rate coefficients. © 2010 American Institute of Physics. [doi:10.1063/1.3457940]

I. INTRODUCTION

Since the 1950s the recombination of H$_3^+$ ions with electrons has been considered one of the most important problems in recombination studies because of its fundamental importance for plasma physics, theoretical atomic physics, and astrophysics.[1–10] The problem of H$_3^+$ recombination motivated many theoretical and experimental studies when the infrared absorption spectrum of H$_3^+$ was observed[11] and H$_3^+$ was discovered in the auroral regions of Jupiter[12] and in the interstellar space.[13,14]

Before the year 2001, no theoretical explanation existed for the relatively fast rate of recombination of H$_3^+$ with electrons that was observed in most experiments with H$_3^+$.[15–19] In addition, there was a significant difference in recombination rate coefficients obtained in different experiments.[17,20] The spectroscopic experiments with H$_3^+$ did not solve the problem.[21–24] Up to now, the spectroscopic study of D$_3^+$ recombination has not been reported at all.

The understanding of the main mechanism of binary dissociative recombination (DR) of H$_3^+$ and D$_3^+$ improved when the Jahn–Teller coupling was included in the theory.[25–28] For a plasma in thermodynamic equilibrium the obtained theoretical values of the binary rate coefficients of the DR of H$_3^+$ and D$_3^+$ ions are $\alpha_{H_3^+}(300 \text{ K})=5.6\times10^{-8}$ cm^3 s^{-1} and $\alpha_{D_3^+}(300 \text{ K})=4\times10^{-8}$ cm^3 s^{-1}, respectively.[29,30] The theory of DR predicted for H$_3^+$ (and isotopologues)[26,27,31,32] that the cross-sections depend on the rotational excitation of the ions. In addition, it was shown[27,32–34] that electron-ion collisions can cause rotational excitation and de-excitation of the ion with a high probability. In recent storage-ring experiments with cold H$_3^+$ ion sources the recombination rate coefficients

obtained agree well with the theoretical predictions.[35,36] In the Heidelberg TSR experiment,[37] the DR cross-section obtained for paraenriched H$_3^+$ at low collision energies was found to be larger than the cross-section for "normal" ortho-/paramixture. These results have been confirmed in recent CRYRING experiments in Stockholm.[38] We have to mention here that there is no direct (*in situ*) determination of the state population of recombining ions in the storage rings. Up to now, no storage-ring measurement with cold and state selected D$_3^+$ has been carried out.

We have studied the recombination of both H$_3^+$ and D$_3^+$ ions with electrons in several plasma experiments: Advanced Integrated Stationary Afterglow (AISA) (Refs. 6, 7, 39, and 40) and several modifications of the Flowing Afterglow with Langmuir Probe (FALP).[41–43] It was found that the measured recombination rate coefficients depend on the H$_2$ (and D$_2$) densities.[6,7,39–43] By measuring the He-pressure dependence, we came to the conclusion that, in conditions typical for afterglow experiments (77–300 K and 100–2000 Pa), the recombination of H$_3^+$ and D$_3^+$ ions with electrons is not a pure binary process;[44–46] helium and molecular hydrogen participate as the third body in H$_3^+$+e^- and D$_3^+$+e^- recombination.

The main focus of the present paper is the recombination process in a D$_3^+$-dominated afterglow plasma. The observed plasma "deionization" can be described by an apparent (effective) binary recombination rate coefficient, $\alpha_{eff}=\alpha_{eff}(T,[D_2],[He])$.[44–46] The index "eff" stresses the fact that we measure the "effective binary recombination rate coefficient" from the rate of plasma deionization. The measured dependence of α_{eff} on $[D_2]$ and $[He]$ suggests that the observed deionization process may involve several parallel and competing channels.

The sequence of collisions leading to recombination can start with (D$_3^+$+D$_2$), (D$_3^+$+He), or (D$_3^+$+e^-) collision. Colli-

---

a)Electronic mail: radek.plasil@mff.cuni.cz.

sions and $(D_3^+ + e^-)$ are discussed in detail below. The $(D_3^+ + D_2)$ collisions can lead to the formation of the intermediate van der Waals molecular ion $D_3^+ \cdot D_2$ which can be stabilized in a low temperature plasma (the process known as ternary association, see, e.g., Ref. 43, 47, and 48). After the D_5^+ ion is formed, the process of "deionization" is terminated by a fast dissociative recombination between D_5^+ and e^-. The process has been discussed quantitatively in previous studies.[41,43,48–50] Formation of $D_3^+ \cdot \text{He}$ is not considered because of its low dissociation energy.

Neutral unstable D_3 and H_3 molecules have been observed many times in plasmas.[51,52] The lifetimes of certain electronic states of D_3 and H_3 molecules were calculated[53] and measured.[54] Only certain electronic states of D_3 can be populated due to collisions $D_3^+ + e^-$. Our calculations suggest that at low electron energies long-lived highly excited neutral D_3^* (molecular Rydberg states) can be formed. This can lead to ternary recombination in plasma. We found experimentally that the recombination of D_3^+ plasma depends also on the helium density at 200–300 K.[46] In the present study we have extended our measurements down to 77 K.

Ternary electron-ion recombination was predicted by Thomson[55] and by Bates and Khare[56] and observed in experiments.[57–59] The ternary recombination of D_3^+ and H_3^+ ions observed in our studies can be, depending on the temperature, more effective than their estimate by a factor of 100. It is an essentially different process than the process considered by Thomson. The large rate coefficients of the observed ternary recombination of D_3^+ and H_3^+ are mainly due to the long autoionization lifetimes of highly excited Rydberg molecules formed in collision between D_3^+ (or H_3^+) and electrons at low temperatures.

II. EXPERIMENTS

Several modifications of flowing afterglow experiments were used in the presented work (see description in Refs. 43 and 60–62). The Cryo-FALP designed to operate at temperatures in the range 77–300 K and at helium pressure 200–2000 Pa was constructed and used for low temperature studies. In Cryo-FALP, the plasma is created in the upstream glass section of the flow tube (at 300 K) in the microwave discharge (10–30 W) in pure helium. Because of the high pressure, He^+ ions formed in the discharge react in a three-body association reaction forming a He_2^+-dominated plasma. Downstream from the discharge, Ar is added and the plasma becomes Ar^+ dominated (see details of the formation in Refs. 7, 39, and 43).

Metastable He atoms formed in the discharge are removed from the afterglow by Penning ionization when Ar is added (see Refs. 7 and 63). Via the second entry port (35 ms downstream from the Ar entry port), D_2 is introduced into the already relaxed cold plasma. In a sequence of ion-molecule reactions, the D_3^+ dominated plasma is formed. A numerical model is used to simulate the processes along the flow tube. Analysis of the data calculated for $[D_2] = 2.4 \times 10^{12}$ cm^{-3} reveals that D_3^+ becomes the dominant ion in the decaying plasma approximately 2 ms after D_2 is added. Argon plays a role in plasma relaxation and in the formation

of D_3^+ but after the D_3^+-dominated plasma is formed, Ar does not participate in ion chemistry anymore. Only at very high $[\text{Ar}]$, the clusters $D_3^+ \cdot \text{Ar}$ can be formed.[64] In the present experiments we are using low Ar densities so we can neglect the formation of $D_3^+ \cdot \text{Ar}$. Note that formed D_3^+ has several collisions with D_2 prior to its recombination so we can expect quenching of eventual internal excitation of D_3^+ ions gained from exothermicity of forming reactions (see also discussion below).

Downstream from the Ar entry port the flow tube is cooled by liquid nitrogen to the required temperature. An axially movable Langmuir probe[63,65] is used to monitor the electron density decay downstream from the deuterium entry port. This probe was calibrated by the well-known rate coefficient of O_2^+ recombination.[5] In fact, the calibration just confirmed accuracy of electron density measurements based on probe theory (see also the discussion in Refs. 6, 7, 42, 62, and 65–67).

Although the plasma decay in D_3^+ dominated plasma is governed by several parallel recombination processes, we introduce a single parameter of the decay—the effective apparent binary recombination rate coefficient α_{eff}. The decay can then be described by the balance equation:

$$\frac{dn_e}{dt} = -\alpha_{\text{eff}} n_i n_e - \frac{n_e}{\tau_D} = -\alpha_{\text{eff}} n_e^2 - \frac{n_e}{\tau_D}, \qquad (1)$$

where n_e and n_i are electron and ion densities. We assume that the plasma is quasineutral ($n_e = n_i$) and the constant τ_D characterizes the ambipolar diffusion during the afterglow. In the experiments we used He and D_2 densities in the interval $[\text{He}] \approx 6 \times 10^{16} - 6 \times 10^{17}$ cm^{-3} and $[D_2] \approx 10^{11} - 10^{15}$ cm^{-3}. Analyzing dependencies of α_{eff} on $[\text{He}]$ and $[D_2]$ and on temperature we have obtained $\alpha_{\text{eff}} = \alpha_{\text{eff}}(T, [D_2], [\text{He}])$.

III. EXPERIMENTAL RESULTS

To obtain effective recombination rate coefficients we measured the electron density decay along the flow tube in a $\text{He}/\text{Ar}/D_2$ mixture. A few examples of decay curves, measured in the D_3^+ dominated afterglow plasma at 77 K and at several D_2 densities, are plotted in panel (a) of Fig. 1. The dependence of the decay rate on $[D_2]$ is evident (see discussion in Refs. 7, 39, and 44–46). Some examples of decay curves measured at higher temperatures are plotted in panel (b) of Fig. 1.

In Fig. 2 the measured effective binary recombination rate coefficients (α_{eff}), are plotted as functions of $[D_2]$. We also show the data previously obtained in other experiments. Below we discuss in detail the data plotted in the figure.

Panel (a) of Fig. 2:

(1) 77 K; *Cryo-FALP*. At a fixed flow tube temperature $T = 77$ K and at $[\text{He}] = 2.1 \times 10^{17}$ cm^{-3} the dependence of α_{eff} on $[D_2]$ was measured in the interval 3×10^{11} cm$^{-3} < [D_2] \lesssim 4 \times 10^{13}$ cm^{-3}. For two other helium densities, α_{eff} was measured only over a limited range, $[D_2] \approx (2-10) \times 10^{12}$ cm^{-3}. The measured dependencies have a plateau where α_{eff} is independent on $[D_2]$. Notice that the data obtained at different $[\text{He}]$ overlap, indicating that at 77 K the dependence of α_{eff}
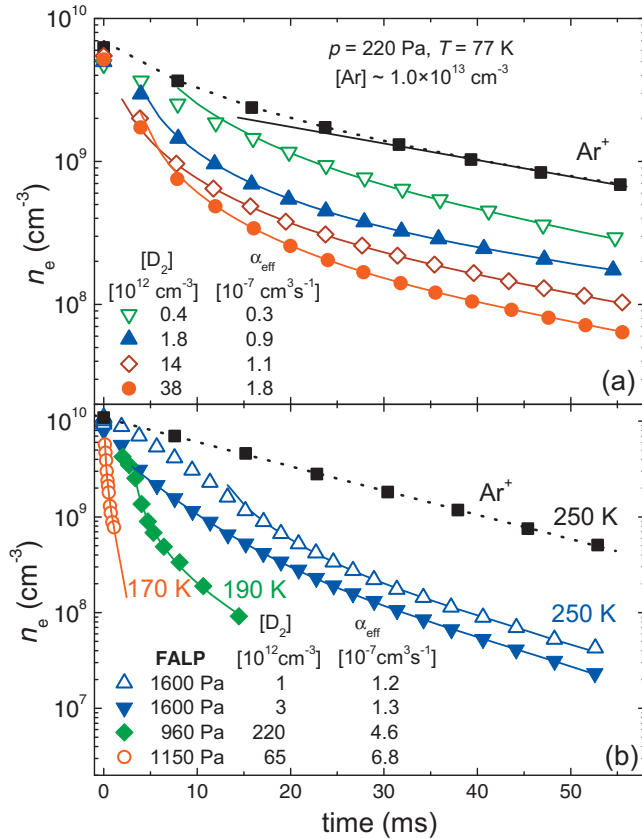
FIG. 1. Electron density decays measured in D$_3^+$ dominated afterglow plasma in the He/Ar/D$_2$ mixture. (a) Data measured at 77 K and 220 Pa. The decay curve measured in Ar$^+$ plasma is also given. (b) Data measured with several modifications of the FALP geometry. He pressures and temperatures are indicated. The decay curve measured in an Ar$^+$ plasma (250 K with) is also shown.

on [He] is very small. At 77 K we have also measured decay of the Ar$^+$ dominated plasma [see panel (a) of Fig. 1]. If the plasma decay was due to ambipolar diffusion only, we would observe an exponential decay,
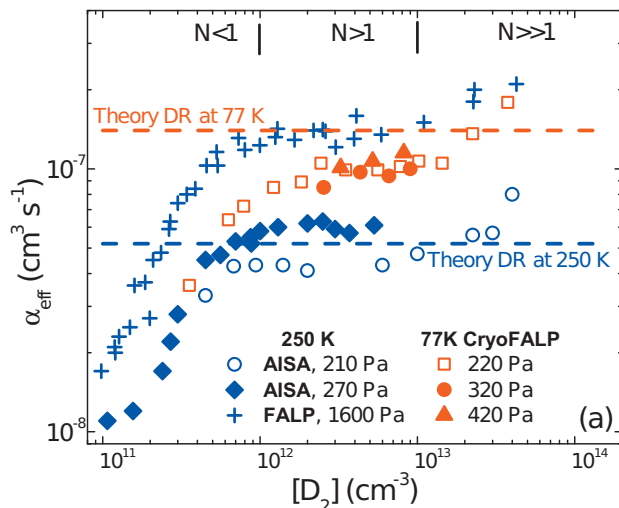
similar to the one observed for Ar$^+$ ions at 250 K [the linear decay curve in semilogarithmic plot on panel (b) of Fig. 1]. The faster decay in the early afterglow indicates an additional loss mechanism. We assign it to the process of collisional radiative recombination (CRR) of Ar$^+$ ions.[68,69] The obtained ternary rate coefficient from this fast decay is equal to the value calculated for the CRR rate coefficient at temperature (85 ± 10) K. This is an additional confirmation that the electron temperature in the afterglow plasma in Cryo-FALP is relaxed and is close to the buffer gas temperature (77 K).

(2) 250 K; *AISA*. Examples of data measured with AISA at 210 and 270 Pa. The data were measured as a function of the deuterium density.[7,39] *FALP*. Examples of data measured with FALP at pressure 1600 Pa. Some decay curves are plotted in panel (b) of Fig. 1. Notice the large dependence on pressure.

(3) 77 and 250 K [and 300 K in panel (b)]; *theory of DR*. The α_{DR} have been calculated under the assumption that ions are in thermodynamic equilibrium.[27,30]

Panel (b) of Fig. 2:

(1) 170, 190, and 260 K; *FALP*. The data were obtained at pressures 700–2000 Pa.[43] The experiment was aiming to understand recombination in a mixture of D$_3^+$ and D$_5^+$ ions. By changing [D$_2$] the ratio [D$_3^+$]/[D$_5^+$] also changes. From the measured α_{eff} we obtained recombination rate coefficients for the both ions.[43] To obtain α_{eff} for D$_3^+$ ions we used linear plots and the limit for [D$_2$]→0 (see the inset).

(2) 300 K; *Cryo-FALP*. α_{eff} measured over a limited interval of [D$_2$] at two He pressures (1020 and 1980 Pa). In FALP experiments at 300 K of Gougousi *et al.*[70] and Laubé *et al.*,[71] the data were obtained at relatively high [D$_2$] (see Fig. 3 in Ref. 46).

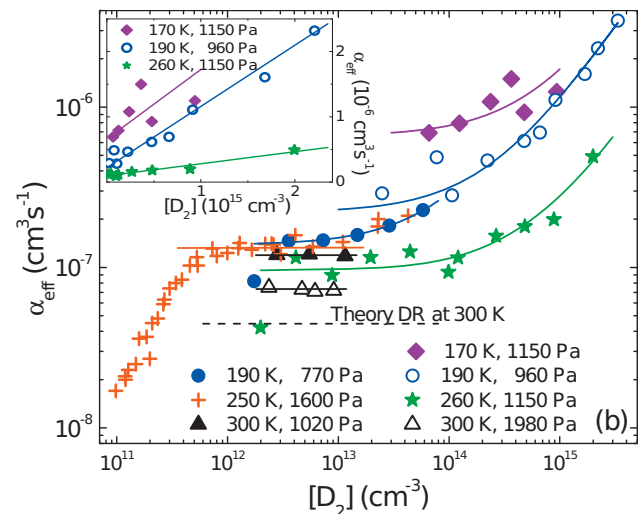In the experiments the [D$_2$] was varied in the interval

FIG. 2. D$_3^+$ effective binary recombination rate coefficient α_{eff} as a function of the deuterium density. (a) The data measured with Cryo-FALP (77 K), AISA (250 K) (Refs. 7 and 39) and FALP (250 K) (Ref. 45). (b) The FALP data obtained at 170, 190, 260, and 300 K (high [D$_2$]). The inset shows the same plot on a linear scale. Such plots were used for the linear extrapolation toward low [D$_2$] corresponding to "region of saturation" (Ref. 43). The FALP data with low [D$_2$] are also shown (250 K). The theoretical values of DR rate coefficient α_{DR} for 77, 250, and 300 K are also plotted (Ref. 30).
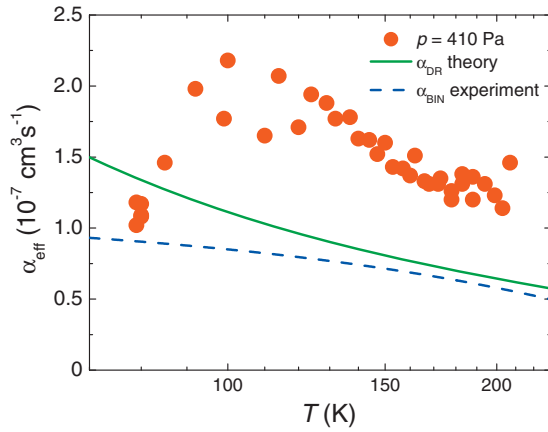
FIG. 3. The effective recombination rate coefficient (α_{eff}) measured in the Cryo-FALP experiment with continuous slow increase of temperature. The partial pressures of He and D_2 were kept constant during the measurements. The densities at 77 K are $[He] = 3.8 \times 10^{17}$ cm^{-3} and $[D_2] = 2.6 \times 10^{12}$ cm^{-3}. The theoretical α_{DR} (Refs. 27 and 30) and experimental α_{Bin} values for the binary electron-D_3^+ dissociative recombination are also given.

10^{11} cm$^{-3} < [D_2] < 10^{15}$ cm^{-3}. In certain measurements α_{eff} was measured only over a limited interval of $[D_2]$. Figure 2 provides information on the dependence of α_{eff} on temperature and on [He] and $[D_2]$. It is evident from Fig. 2 that the measured dependencies on $[D_2]$ clearly reveal three regions with specific dependencies of α_{eff} on $[D_2]$. In addition, we can see clear dependencies of α_{eff} on [He] and on temperature.

Below, we discuss recombination in plasma at such $[D_2]$ for which α_{eff} is nearly independent on $[D_2]$, i.e., 10^{12} cm$^{-3} < [D_2] < 10^{14}$ cm^{-3}, "the region of saturation." At such $[D_2]$ the D_3^+ ion undergoes several collisions with D_2 before it recombines with an electron. To demonstrate this we compare the characteristic time for recombination with the characteristic time of interaction with D_2. The number of interactions with D_2, in Fig. 2(a) indicated by N, could be estimated if we consider only the collisions leading to a change in the nuclear spin of D_3^+, for which the rate coefficients are known,[9,30,72] $k_{SCH} \approx 2 \times 10^{-10}$ cm^3 s^{-1}. The frequency ν_{SCH} of these reactions at $[D_2] = 10^{12}$ cm^{-3} is $\nu_{SCH} = k_{SCH} \times [D_2] \approx 200$ s^{-1}. If we use $\alpha_{eff} \approx 1 \times 10^{-7}$ cm^3 s^{-1}, the recombination frequency is $\nu_{rec} = \alpha_{eff} \times n_e \approx 200$ s^{-1} at the typical FALP conditions where $n_e \approx 2 \times 10^9$ cm^{-3}. For $[D_2] > 10^{12}$ cm^{-3} and $n_e < 2 \times 10^9$ cm^{-3} we obtain $\nu_{SCH} > \nu_{rec}$.

Using Cryo-FALP we have also carried out measurements, in which the flow tube was first cooled by liquid nitrogen down to 77 K and then the flow of liquid nitrogen was stopped and the temperature of the flow tube was slowly increasing up to 210 K. At fixed buffer gas pressure α_{eff} was measured as a function of the actual flow tube temperature. The obtained data are plotted in Fig. 3. A sharp increase of α_{eff} with the increasing temperature starting from 77 K was observed. When the temperature becomes larger than ≈ 100 K, α_{eff} starts to decrease.

IV. ANALYSIS OF THE EXPERIMENTAL RESULTS

In this section we analyze the dependence of α_{eff} on [He] in the "region of saturation," 10^{12} cm$^{-3} < [D_2] < 10^{14}$ cm^{-3}.
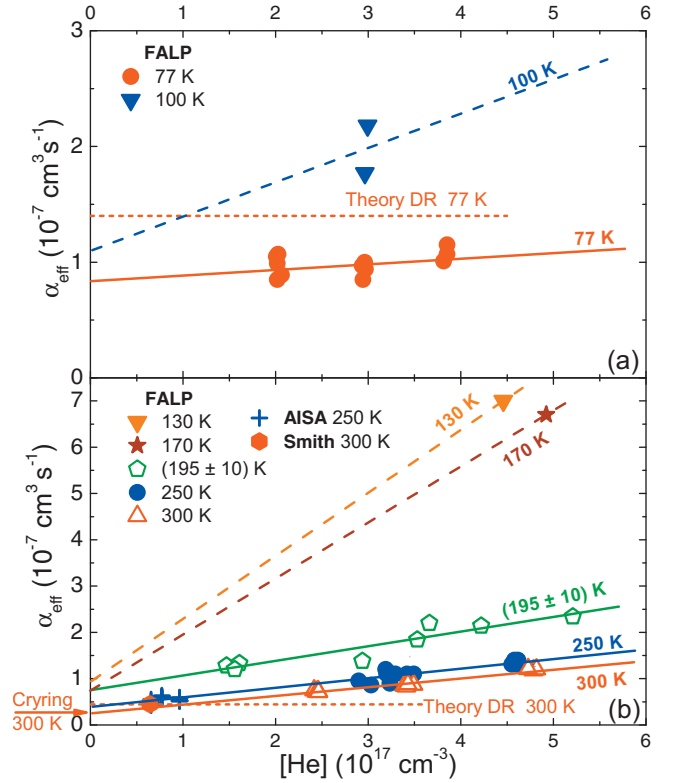

FIG. 4. Dependencies of the effective binary recombination rate coefficient (α_{eff}) on [He] measured at different temperatures. The data were obtained at deuterium densities: 10^{12} cm$^{-3} < [D_2] < 10^{14}$ cm^{-3} (region of saturation). The figures includes also the data from previous AISA experiments (Ref. 39) and the value obtained by Smith and Spanel in a FALP experiment (Ref. 17). Data for 250, 300, and partly for 195 K are taken from Ref. 46. Theoretical values for 300 and 77 K are indicated by horizontal dashed lines (Ref. 30). The experimental value (Refs. 73 and 74) obtained in CRYRING and corresponding to 300 K is indicated by an arrow (Cryring 300 K).

In order to obtain the dependence of α_{eff} on [He], we plotted α_{eff} measured at a constant temperature versus [He] (see Fig. 4). At 250 and 300 K, we measured the dependence of α_{eff} on [He] explicitly [see panel (b) in Fig. 4]. For (195 ± 10) K we have performed several measurements, including the one obtained directly as a function of [He]. On the corresponding plots we can see a clear linear dependence of α_{eff} on [He] (full straight lines). The dependence of α_{eff} on [He] at 77 K was also measured explicitly. For temperatures 100, 130, and 170 K, we have measured α_{eff} only for certain values of [He].

If we assume that the D_3^+-dominated plasma recombination is governed by the binary $(D_3^+ + e^-)$ and ternary $(D_3^+ + e^- + He)$ processes, the effective recombination rate can be represented as

$$\alpha_{eff} = \alpha_{Bin}(T) + K_{He}(T) \cdot [He], \qquad (2)$$

where $\alpha_{Bin}(T)$ is the effective rate coefficient for the binary recombination and $K_{He}(T)$ is the effective rate coefficient for the ternary recombination.

The α_{Bin} obtained from the measured [He]-dependencies of α_{eff} (solid lines in Fig. 4) are plotted in Fig. 5 as a function of temperature. The agreement between the measured value $\alpha_{Bin}(T)$, the calculated value $\alpha_{DR}(T)$, and the CRYRING data is very good. A linear extrapolation of the measured $\alpha_{Bin}(T)$
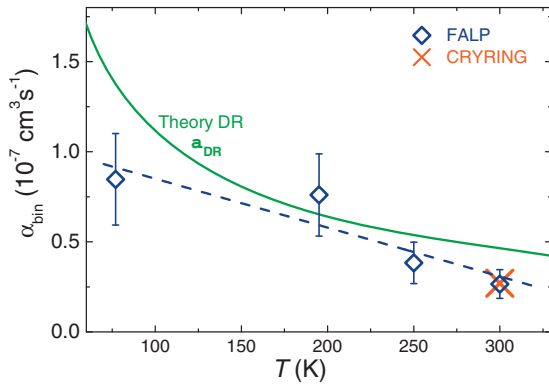
FIG. 5. D$_3^+$ binary recombination rate coefficients. The solid line indicates the calculated values for the binary dissociative recombination (α_{DR}) at a thermal population of the para-/ortho-/metastates of D$_3^+$ (Ref. 30). The values α_{Bin} (diamonds) were obtained from measured $\alpha_{eff}(T,[He])$. The dashed line is a fit to the experimental data. The experimental value (Refs. 73 and 74) from the CRYRING experiment is shown by a cross (×).

has been used to derive $K_{He}(T)$ from the measured $\alpha_{eff}(T)$ (see dashed lines in Fig. 4). The obtained values of $K_{He}(T)$ are plotted in Fig. 6 as a function of temperature. We briefly summarize the data plotted in Fig. 6.

(1) 77 K; Cryo-FALP (closed diamond). Data obtained in the present experiments by measuring the pressure dependence of α_{eff} at 77 K (see Fig. 4). Actually, we have observed only a very small pressure dependence $K_{He}(77\ K) \approx 0.5 \times 10^{-25}$ cm^6 s^{-1}.

(2) 130 and 170 K; FALP (triangles). The experiments were carried out using the flow tube with a small diameter. A fast flow of the buffer gas is well suited for studying fast plasma decays (see decay curve for 170 K in Fig. 1). We have measured the dependence of α_{eff} on [D$_2$] but only at one fixed [He]. To obtain K_{He}, we have used the extrapolated value of $\alpha_{Bin}(T)$ as discussed above (the dashed line in Fig. 5).
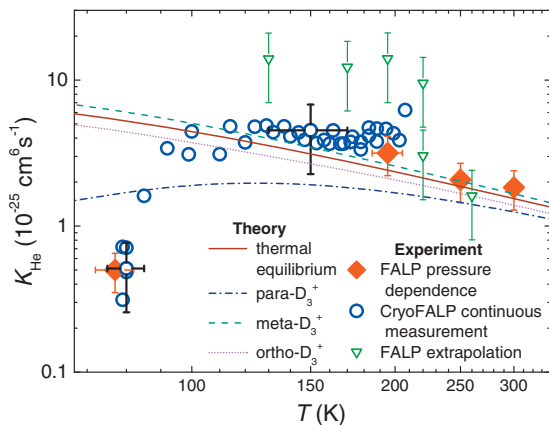

FIG. 6. The ternary recombination rate coefficient, $K_{He}(T)$, for He assisted recombination of D$_3^+$ ions. The values obtained from the measured linear dependencies of effective recombination rate coefficient on [He] (see full lines in Fig. 4) are indicated by diamonds. The values of K_{He} obtained at a fixed He density and a fixed temperature using the extrapolated values of $\alpha_{Bin}(T)$ are shown by triangles. The data measured with Cryo-FALP with the continuously increasing temperature are indicated by circles (see the text and Fig. 3). We have also specified theoretical ternary rate coefficients for ortho-, para-, and meta-D$_3^+$ as well as the value calculated for the thermal ortho-/para-/meta-D$_3^+$ equilibrium (Ref. 46).

(3) 190, 220, and 260 K; FALP (triangles). α_{eff} measured in different experiments (see Fig. 2, panel b). To obtain K_{He} we have used $\alpha_{Bin}(T)$.

(4) 195, 250, and 300 K; FALP (closed diamonds). The data from the pressure dependence of α_{eff}, see panel (b) of Fig. 4 (see also Ref. 46).

(5) 77–210 K; "Continuous measurement" with Cryo-FALP (open circles). We measured $\alpha_{eff}(T)$ by continuously increasing the flow tube temperature. From the measured $\alpha_{eff}(T)$ we calculated $K_{He}(T)$ using $\alpha_{Bin}(T)$.

The ternary recombination rate coefficients calculated for different spin states are also plotted in the Fig. 6. The calculated and measured values are in good agreement at temperatures above 100 K. The sharp increase of K_{He} observed at temperatures below 100 K is somewhat surprising when comparing with previous studies of ternary association processes,[48,61,75] in which the monotone decrease, $K \sim T^{-n}$, was usually observed. We can also refer to other measurements[69,76] of ternary recombination rate coefficients in which the electron played the role of a third body. In these studies a steep decrease of the rate coefficient with the temperature was observed (CRR, $K \sim T^{-9/2}$). The measured rise of K_{He} is not understood yet.

V. THEORETICAL MODEL FOR HELIUM-ASSISTED TERNARY RECOMBINATION OF D$_3^+$

The theory of the ternary helium assisted recombination of H$_3^+$ and D$_3^+$ ions has been developed and described in our earlier papers[44–46] for the D$_3^+$ recombination. We will give only a short summary here. Low-energy (0–0.3 eV) collisions between an electron and H$_3^+$ (or D$_3^+$) can lead to the rotational excitation of the ion with an appreciable probability (see Table VI in Ref. 27) if the kinetic energy of the incident electron is large enough to excite the ion rotationally. The large probability is caused by a strong coupling between the rotating ionic core (H$_3^+$ or D$_3^+$) and the motion of the incident electron. For a given total angular momentum N of the ion+electron system, the scattering amplitude for a p-wave electron incident on the ion depends strongly on the projection $\Lambda = 0, \pm 1$ ($p\sigma$ and $p\pi$ electronic states) of the electronic angular momentum ($l=1$) on the molecular symmetry axis. When the electron is close to the ion, the energy of the system is determined by the electronic states of the molecule. Correspondingly, the scattering matrix is diagonal if one considers the scattering from the ion with clumped nuclei. At an infinite separation between the ion and the electron, the appropriate scattering channels are determined not by Λ but by the rotational states of the ionic core, i.e., by quantum numbers (N^+, K^+). Here and below N^+ and K^+ are the angular momentum of the ion and its projection on the molecular symmetry axis. The quantum states with definite (N^+, K^+) are linear combinations of states with different Λ. Our treatment here considers only rotational transitions (without changing the vibrational level of the ion, which is assumed to be the lowest vibrational level). In this situation, the states with definite (N^+, K^+) and Λ are linked to each other by Clebsch–Gordan coefficients (rotational frame transformation). For more detail, see Refs. 27 and 32. Be-

cause the scattering matrix at small ion-electron separations is diagonal with very different diagonal elements (we do not consider here the Jahn–Teller physics, which is inactive if the initial and final vibrational levels of the ion are the same), the scattering matrix in the representation describing the $N^+ \rightarrow N^{+'} = \pm 1$ or $N^+ \pm 2$ change in the rotational state has appreciable nondiagonal matrix elements. Therefore, the probability for the $N^+ \rightarrow N^{+'} = \pm 1$ or $N^+ \pm 2$ transitions could be comparable to the unity. If the ion is in its lowest rotational state and the electronic kinetic energy is not sufficient for such a $N^+ \rightarrow N^{+'}$ transition, the large difference in the scattering phases between $p\pi$ and $p\sigma$ states is transformed into a large probability of transition from the open (N^+) into the closed $(N^{+'})$ channel. In such a situation, the presence of a closed channel is manifested as an appearance of a series of autoionizing Rydberg resonances (Beutler–Fano resonances) with large widths in spectra of different observables (such as photoionization). The series converges to the closed $(N^{+'})$ channel. Such a situation with the H_3^+ ion has been observed in photoionization experiments of Helm.[77,78] In these experiments, the Beutler–Fano photoionization parts of the spectrum [between the two coupled rotational levels, (10) and (30), of H_3^+] demonstrate a series of wide Beutler–Fano resonances[79] with widths comparable to the energy difference between the two consecutive resonances. The fact that the widths are comparable with the energy difference between the resonances means that the probability for $N^+ \rightarrow N^{+'}$ transitions in electron-ion collisions is comparable to unity. The theoretical photoionization spectra based on this concept[77,78,80] agree well with the experimental data.

From a time-dependent point of view, the appearance of resonances in spectra corresponds to a long $D_3^+ + e^-$ collision time. For collision energies between two coupled rotational levels of D_3^+ [for example between the (00) and (20) levels], the delay time in electron-ion collisions is increased and may be long enough to be comparable with the time between two consecutive collisions of the $D_3^+ + e^-$ system with background helium atoms. From a time-independent point of view, in a low-temperature gas containing electrons and D_3^+ ions, the probability that a helium atom collides with a weakly bound D_3^* Rydberg molecule is significant because the electronic probability density in D_3^* is greatly increased near the ionic core due to the strong interaction of the closed channel of the D_3^* complex with the entrance channel of the $D_3^+ + e^-$ system.

As a result of this qualitative view of the process, we have developed in Refs. 44–46 a two-step model for the helium-assisted recombination of D_3^+ (and H_3^+) with electrons. First, D_3^+ and an e^- collide and form a rotationally autoionizing resonance $D_3^*(np)$. Then a collision with a helium atom changes the electron state of $D_3^*(np)$ to a state $D_3^*(nl)$ with a different $(l \neq 1)$ electronic angular momentum that makes autoionization impossible and eventually leads to the dissociation. This can be written as

$$(\text{step } 1) \quad D_3^+ + e^- \rightarrow D_3(np), \tag{3}$$

$$(\text{step } 2) \quad D_3(np) \xrightarrow{\text{He}} D_3(nl) \rightarrow \begin{cases} D_2 + D \\ D + D + D. \end{cases} \tag{4}$$
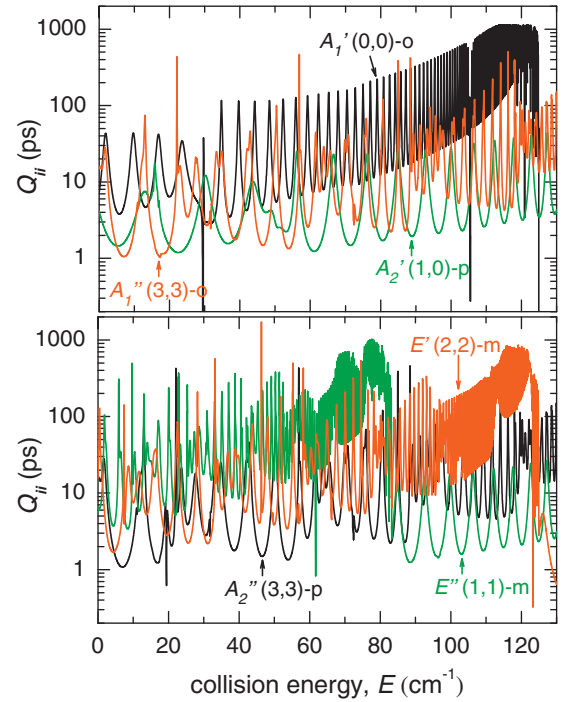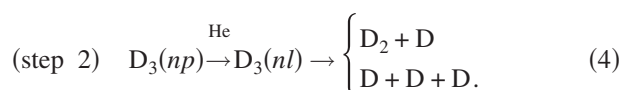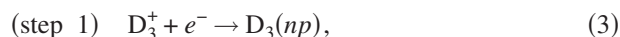

FIG. 7. The diagonal elements $Q_{ii}(E_1)$ of Smith's lifetime matrix calculated from the scattering matrix as discussed in Ref. 46 for the six different irreducible representations of the $K_{He}(T)$ system. Each of the six curves shown in the figure is labeled with the corresponding symbol of irreducible representation (A_1', A_2', etc.) and the rotational quantum numbers (N^+, K^+) of the ion followed by -o, -m, or -p (for ortho-, meta-, or para-D_3^+).

The rate constant $K_i^{3D}(E_1, E_2)$ for the two-step process above depends on the energy E_1 of collision between e^- and D_3^+, on the energy E_2 of collision between D_3^* and He, and on the initial state $|i\rangle$ of D_3^+. The formula for $K_i^{3D}(E_1, E_2)$ is derived in Ref. 45 (in a.u.),

$$K_i^{3D}(E_1, E_2) = \frac{\pi}{\sqrt{2E_1}} Q_{ii}(E_1) k^l(E_2), \tag{5}$$

where $Q_{ii}(E_1)$ is the diagonal element of Smith's lifetime matrix,[81] $k^l(E_2)$ is the rate constant for the second step of the process, $k^l(E_2) = \sqrt{2E_2/m_2}\sigma(E_2)$, $\sigma(E_2)$ is the cross-section for the second reaction in Eq. (4), and m_2 is the reduced mass of the D_3^*-He system.

The lifetime matrix elements $Q_{ii}(E_1)$ in Eq. (5) depend strongly on the energy E_1 and on the initial state of the electron-ion system. A few examples of the energy-dependence of $Q_{ii}(E_1)$ for several different initial states $|i\rangle$ are shown in Fig. 7. The figure shows the $Q_{ii}(E_1)$ elements for the all six irreducible representations of the $D_3^+ + e^-$ system (A_1', A_1'', A_2', A_2'', E', and E'') at low collisional energies. Most of the resonances shown are due to the Rydberg series of autoionizing electronic states converging to the first excited rotational state of the corresponding irreducible representation. As one can see from the figure, in addition to the regular Rydberg series of resonances, there are resonances perturbing the series. These perturbers belong to highly excited ionization limits.

In order to compare theory with the present experiment, the rate constant K_i^{3D} should be averaged with respect to

Maxwell–Boltzmann distributions over collisional energies E_1 and E_2, and with respect to initial population of ionic states $|i\rangle$ at a given temperature T,

$$\langle K^{3D} \rangle = \sqrt{\frac{2\pi}{(k_B T)^3}} \frac{k^l \Sigma_i \int_0^\infty Q_{ii}(E_1) w_i \exp(-E_1 + E_i/k_B T) dE_1}{\Sigma_i w_i \exp(-E_i/k_B T)}, \tag{6}$$

where $k^l = k^l(E_2)$ is assumed to be energy independent, w_i and E_i are the statistical weight and energy of the initial state $|i\rangle$ of the D$_3^+$ ion, and k_B is the Boltzmann constant.[45] The thermally averaged rate coefficient $\langle K^{3D} \rangle$ obtained is shown in Fig. 6.

VI. DISCUSSION AND CONCLUSIONS

This is the fourth in the present series of papers devoted to the study of ternary and binary recombinations of H$_3^+$ and D$_3^+$ ions with electrons. In previous papers we described experimental data for H$_3^+$ recombination and data for D$_3^+$ recombination at 200–300 K.[46] In the present paper we have extended the previous D$_3^+$ study down to 77 K. The binary recombination rate coefficients measured in the present experiments are in good agreement with data calculated for binary dissociative recombination[27,28,30] and with available storage ring data.[73,74]

We have also developed the theoretical model describing process of the observed helium assisted ternary recombination. In this model we consider the helium-assisted recombination as a two-step process (two rate determining steps). First, the ion and electron collide forming a relatively long-living autoionizing resonance D$_3^*$(np) with the rotationally excited ionic core. Then a collision with a helium atom changes the electronic state of D$_3^*$(np) to a state D$_3^*$(nl) with a different ($l \neq 1$) electronic angular momentum. To support this model we calculated lifetime (delay time) of D$_3^*$(np) formed in electron-ion interaction. Calculations showed that at temperatures 77–300 K the lifetime can be as large as a few hundreds of picoseconds. The obtained delay times were used to calculate ternary recombination rate coefficients and their temperature dependence. The calculated values are in agreement with the measured values at higher temperatures (100–300 K) but the theoretical model does not describe correctly the observed suppression of ternary recombination at lower temperatures. The disagreement might indicate that at low temperatures the rate coefficients k^l are not energy independent (see, e.g., theory and compilation of data by Hickman in Ref. 82).

There are still many open questions concerning the process of recombination of H$_3^+$ and D$_3^+$ ions. One of the most important questions now is the state selectivity at low temperatures.

ACKNOWLEDGMENTS

[1] T. Oka, Philos. Trans. R. Soc. London, Ser. A **358**, 2363 (2000).
[2] E. Herbst, Philos. Trans. R. Soc. London, Ser. A **358**, 2523 (2000).
[3] R. Johnsen, J. Phys.: Conf. Ser. **4**, 83 (2005).
[4] E. Shkolnik, E. Gaidos, and N. Moskovitz, Astrophys. J. **132**, 1267 (2006).
[5] M. Larsson and A. Orel, *Dissociative Recombination of Molecular Ions* (Cambridge University Press, New York, 2008).
[6] J. Glosík, R. Plasil, V. Poterya, P. Kudrna, and M. Tichy, Chem. Phys. Lett. **331**, 209 (2000).
[7] R. Plasil, J. Glosik, V. Poterya, P. Kudrna, J. Rusz, M. Tichy, and A. Pysanenko, Int. J. Mass Spectrom. **218**, 105 (2002).
[8] T. R. Geballe and T. Oka, Science **312**, 1610 (2006).
[9] D. Gerlich, F. Windish, P. Hlavenka, R. Plasil, and J. Glosik, Philos. Trans. R. Soc. London, Ser. A **364**, 3007 (2006).
[10] M. Larsson, B. McCall, and A. E. Orel, Chem. Phys. Lett. **462**, 145 (2008).
[11] T. Oka, Phys. Rev. Lett. **45**, 531 (1980).
[12] L. Trafton, D. Lester, and K. Thompson, Astrophys. J. **343**, L73 (1989).
[13] S. Miller, J. Tennyson, S. Lepp, and A. Dalgarno, Nature (London) **355**, 420 (1992).
[14] T. Geballe and T. Oka, Nature (London) **384**, 334 (1996).
[15] N. G. Adams, D. Smith, and E. Alge, J. Chem. Phys. **81**, 1778 (1984).
[16] T. Amano, Astrophys. J. **329**, L121 (1988).
[17] D. Smith and P. Spanel, Int. J. Mass Spectrom. Ion Process. **129**, 163 (1993).
[18] R. Johnsen and J. Mitchell, in *Advances in Gas Phase Ion Chemistry*, Vol. 3, edited by N. G. Adams and L. M. Babcock (JAI Press, Greenwich, CT, 1998), p. 49.
[19] A. Orel, I. Schneider, and A. Suzor-Weiner, Philos. Trans. R. Soc. London, Ser. A **358**, 2445 (2000).
[20] D. Smith and P. Spanel, Chem. Phys. Lett. **211**, 454 (1993).
[21] T. Amano, J. Chem. Phys. **92**, 6492 (1990).
[22] N. Feher, A. Rohrbacher, and J. P. Maier, Chem. Phys. **185**, 357 (1994).
[23] P. Macko, G. Bano, P. Hlavenka, R. Plasil, V. Poterya, A. Pysanenko, O. Votava, R. Johnsen, and J. Glosik, Int. J. Mass Spectrom. **233**, 299 (2004).
[24] J. Glosik, P. Hlavenka, R. Plasil, F. Windisch, D. Gerlich, A. Wolf, and H. Kreckel, Philos. Trans. R. Soc. London, Ser. A **364**, 2931 (2006).
[25] V. Kokooouline, C. H. Greene, and B. D. Esry, Nature (London) **412**, 891 (2001).
[26] V. Kokooouline and C. H. Greene, Phys. Rev. Lett. **90**, 133201 (2003).
[27] V. Kokooouline and C. H. Greene, Phys. Rev. A **68**, 012703 (2003).
[28] C. Jungen and S. T. Pratt, Phys. Rev. Lett. **102**, 023201 (2009).
[29] S. Fonseca dos Santos, V. Kokooouline, and C. H. Greene, J. Chem. Phys. **127**, 124309 (2007).
[30] L. Pagani, C. Vastel, E. Hugo, V. Kokooouline, C. H. Greene, A. Bacmann, E. Bayet, C. Ceccarelli, R. Peng, and S. Schlemmer, Astron. Astrophys. **494**, 623 (2009).
[31] V. Kokooouline and C. H. Greene, J. Phys.: Conf. Ser. **4**, 74 (2005).
[32] A. Faure, V. Kokooouline, C. H. Greene, and J. Tennyson, J. Phys. B **39**, 4261 (2006).
[33] A. Faure, J. Tennyson, V. Kokooouline, and C. H. Greene, J. Phys.: Conf. Ser. **192**, 012016 (2009).
[34] V. Kokooouline, A. Faure, J. Tennyson, and C. H. Greene, Mon. Not. R. Astron. Soc. **405**, 1195 (2010).
[35] B. J. McCall, A. J. Huneycutt, R. J. Saykally, T. R. Geballe, N. Djuric, G. H. Dunn, J. Semaniak, O. Novotny, A. Al-Khalili, A. Ehlerding, F. Hellberg, S. Kalhori, A. Neau, R. Thomas, F. Osterdahl, and M. Larsson, Nature (London) **422**, 500 (2003).
[36] H. Kreckel, M. Motsch, J. Mikosch, J. Glosik, R. Plasil, S. Altevogt, V. Andrianarijaona, H. Buhr, J. Hoffmann, L. Lammich, M. Lestinsky, I. Nevo, S. Novotny, D. A. Orlov, H. B. Pedersen, F. Sprenger, A. S. Terekhov, J. Toker, R. Wester, D. Gerlich, D. Schwalm, A. Wolf, and D. Zajfman, Phys. Rev. Lett. **95**, 263201 (2005).
[37] A. Wolf, H. Kreckel, L. Lammich, D. Strasser, J. Mikosch, J. Glosik, R. Plasil, S. Altevogt, V. Andrianarijaona, H. Buhr, J. Hoffmann, M. Lestinsky, I. Nevo, S. Novotny, D. A. Orlov, H. B. Pedersen, A. S. Terekhov, J.

Toker, R. Wester, D. Gerlich, D. Schwalm, and D. Zajfman, Philos. Trans. R. Soc. London, Ser. A **364**, 2981 (2006).

[38] B. A. Tom, V. Zhaunerchyk, M. B. Wiczer, A. A. Mills, K. N. Crabtree, M. Kaminska, W. D. Geppert, M. Hamberg M. af Ugglas, E. Vigren, W. J. van der Zande, M. Larsson, R. D. Thomas, and B. J. McCall, J. Chem. Phys. **130**, 031101 (2009).

[39] V. Poterya, J. Glosík, R. Plašil, M. Tichý, P. Kudrna, and A. Pysanenko, Phys. Rev. Lett. **88**, 044802 (2002).

[40] J. Glosík, R. Plasil, V. Poterya, P. Kudrna, M. Tichy, and A. Pysanenko, J. Phys. B **34**, L485 (2001).

[41] A. Pysanenko, O. Novotny, P. Zakouril, R. Plasil, V. Poterya, and J. Glosik, Czech. J. Phys. **52**, D681 (2002).

[42] J. Glosík, O. Novotny, A. Pysanenko, P. Zakouril, R. Plasil, P. Kudrna, and V. Poterya, Plasma Sources Sci. Technol. **12**, S117 (2003).

[43] O. Novotný, R. Plasil, A. Pysanenko, I. Korolov, and J. Glosik, J. Phys. B **39**, 2561 (2006).

[44] J. Glosik, I. Korolov, R. Plasil, O. Novotny, T. Kotrik, P. Hlavenka, J. Varju, I. A. Mikhailov, V. Kokoouline, and C. H. Greene, J. Phys. B **41**, 191001 (2008).

[45] J. Glosík, R. Plaŝil, I. Korolov, T. Kotrik, O. Novotný, P. Hlavenka, P. Dohnal, J. Varju, V. Kokoouline, and C. H. Greene, Phys. Rev. A **79**, 052707 (2009).

[46] J. Glosík, I. Korolov, R. Plaŝil, T. Kotrik, P. Dohnal, O. Novotný, J. Varju, S. Roucka, C. H. Greene, and V. Kokoouline, Phys. Rev. A **80**, 042706 (2009).

[47] D. Gerlich and S. Horning, Chem. Rev. (Washington, D.C.) **92**, 1509 (1992).

[48] J. Glosík, G. Bano, E. Ferguson, and W. Lindinger, Int. J. Mass Spectrom. **176**, 177 (1998).

[49] K. Hiraoka and P. Kebarle, J. Chem. Phys. **62**, 2267 (1975).

[50] J. Glosík, V. Skalsky, and W. Lindinger, Int. J. Mass Spectrom. Ion Process. **134**, 67 (1994).

[51] G. Herzberg, Annu. Rev. Phys. Chem. **38**, 27 (1987).

[52] T. Amano and M.-C. Chan, Philos. Trans. R. Soc. London, Ser. A **358**, 2457 (2000).

[53] M. Tashiro and S. Kato, J. Chem. Phys. **117**, 2053 (2002).

[54] I. Mistrík, R. Reichle, H. Helm, and U. Müller, Phys. Rev. A **63**, 042711 (2001).

[55] J. Thomson, Philos. Mag. **47**, 337 (1924).

[56] D. R. Bates and S. P. Khare, Proc. Phys. Soc. London **85**, 231 (1965).

[57] Y. S. Cao and R. Johnsen, J. Chem. Phys. **94**, 5443 (1991).

[58] W. Wolfer, C. Bisson, P. Souers, and R. Tsugawa, Phys. Rev. A **41**, 4470 (1990).

[59] G. Gousset, B. Sayer, and J. Berlande, Phys. Rev. A **16**, 1070 (1977).

[60] A. Florescu-Mitchell and J. Mitchell, Phys. Rep. **430**, 277 (2006).

[61] J. Glosík, P. Zakouril, V. Hanzal, and V. Skalský, Int. J. Mass Spectrom. Ion Process. **149–150**, 187 (1995).

[62] J. Glosík, G. Bánó, R. Plasil, A. Luca, and P. Zakouril, Int. J. Mass Spectrom. **189**, 103 (1999).

[63] I. Korolov, R. Plasil, T. Kotrik, P. Dohnal, O. Novotny, and J. Glosik, Contrib. Plasma Phys. **48**, 461 (2008).

[64] J. Glosík, R. Plasil, A. Pysanenko, O. Novotný, P. Hlavenka, P. Macko, and G. Bánó, J. Phys.: Conf. Ser. **4**, 104 (2005).

[65] J. D. Swift and M. J. R. Schwar, *Electrical Probes for Plasma Diagnostics* (Iliffe, London, 1970).

[66] I. Korolov, T. Kotrik, R. Plasil, J. Varju, M. Hejduk, and J. Glosik, Contrib. Plasma Phys. **48**, 521 (2008).

[67] I. Korolov, R. Plasil, T. Kotrik, P. Dohnal, and J. Glosik, Int. J. Mass Spectrom. **280**, 144 (2009).

[68] E. McDaniel, J. Mitchell, and M. Rudd, *Atomic Collisions, Heavy Particle Projectiles* (Wiley, New York, 1993).

[69] M. Skrzypkowski, R. Johnsen, R. Rosati, and M. Golde, Chem. Phys. **296**, 23 (2004).

[70] T. Gougousi, R. Johnsen, and M. F. Golde, Int. J. Mass Spectrom. Ion Process. **149–150**, 131 (1995).

[71] S. Laubé, A. Le Padellec, O. Sidko, C. Rebrion-Rowe, J. B. A. Mitchell, and B. R. Rowe, J. Phys. B **31**, 2111 (1998).

[72] M. Cordonnier, D. Uy, R. M. Dickson, K. E. Kerr, Y. Zhang, and T. Oka, J. Chem. Phys. **113**, 3181 (2000).

[73] M. Larsson, H. Danared, Å. Larson, A. Le Padellec, J. R. Peterson, S. Rosén, J. Semaniak, and C. Strömholm, Phys. Rev. Lett. **79**, 395 (1997).

[74] A. Le Padellec, M. Larsson, H. Danared, Å. Larson, J. R. Peterson, S. Rosén, J. Semaniak, and C. Strömholm, Phys. Scr. **57**, 215 (1998).

[75] N. G. Adams and D. Smith, *Reactions of Small Transient Species* (Academic, New York, 1983).

[76] D. R. Bates, A. E. Kingston, and R. W. P. McWhirter, Proc. R. Soc. London, Ser. A **267**, 297 (1962).

[77] C. Bordas and H. Helm, Phys. Rev. A **43**, 3645 (1991).

[78] I. Mistrík, R. Reichle, U. Müller, H. Helm, M. Jungen, and J. Stephens, Phys. Rev. A **61**, 033410 (2000).

[79] U. Fano and A. Rau, *Atomic Collisions and Spectra* (Academic, San Diego, California, 1986).

[80] V. Kokoouline and C. H. Greene, Phys. Rev. A **69**, 032711 (2004).

[81] F. T. Smith, Phys. Rev. **118**, 349 (1960).

[82] A. Hickman, Phys. Rev. A **18**, 1339 (1978).